# Interaction force between two finite-size charged particles in weakly ionized plasma

A. I. Momot,[1,*] A. G. Zagorodny,[2,†] and I. S. Orel[3,‡]

[1]*Faculty of Physics, Taras Shevchenko National University of Kyiv, 64/13, Volodymyrs'ka Street, Kyiv 01601, Ukraine*

[2]*M.M. Bogolubov Institute for Theoretical Physics, National Academy of Science of Ukraine, 14b, Metrologichna Street, Kyiv 03680, Ukraine*

[3]*Pierre and Marie Curie University (UPMC), 4 place Jussieu, Paris 75252, France*

(Received 22 November 2016; revised manuscript received 11 January 2017; published 31 January 2017)

The results of numerical studies of the interaction forces between two finite-size charged spherical conductive particles embedded into weakly ionized strongly collisional isothermal plasma-like medium are presented. The studies are performed for the case of particles with fixed electric charge under the assumption that particles do not absorb electrons and ions from the surrounding plasma (colloidal particles) as well as for particles charged by plasma currents (grains). In the first case the Poisson-Boltzmann model was used and in the second the dynamics of grain charging is described in the drift-diffusion approximation. It is shown that at the large distances the interaction force between colloidal particles has the Debye screened asymptotic while for the grains the Coulomb-like behavior is observed. The dependence of the grain charge collected due to the plasma particle absorption on the distance between two grains is studied. The possibility of introducing effective Coulomb description of finite-size grain interaction in weakly ionized strongly collisional plasma is discussed.

DOI: 10.1103/PhysRevE.95.013212

## I. INTRODUCTION

The problem of electrostatic interaction of finite-size charged bodies has a long history [1]. The interaction of charged objects even of spherical form can be described by the Coulomb law for point charges only if their sizes are much smaller than the distance between them. Therefore, the problem arises of calculating the force with which two bodies are repulsed or attracted to each other at arbitrary distances. Recent developments for the case of two conducting spherical particles in a vacuum are presented in Refs. [2–4]. In particular, the repulsion force between like-charged conducting spheres of the same size is less than the Coulomb force for point charges, due to charge polarization. The ratio of these forces reaches the value 0.6149 when the sphere are in contact [3].

Obviously, the presence of plasma around charged finite-size particles considerably complicates the problem under consideration.

At the same time, the knowledge of the force with which two finite-size charged particles interact in plasma is needed for the solution of the verity of problems of dusty plasma physics [5,6] and physics of charged colloidal suspensions [7–10]. These fields of physics deal with the studies of the systems which consist of not only the charged particles that could be treated as point particles (electrons and ions in plasmas and counterions in the case of colloidal suspensions), but also of finite-size charged particles (dust particles, or grains in the case of dusty plasmas and charged colloidal particles in the case of colloidal suspensions). In particular, one of the most important problems in these fields is the description of the ordered structure (for example, dusty and colloidal crystal) formation in dusty plasmas [11,12] and colloidal suspensions [7,8].

It is necessary to note that the problem of grain interaction in dusty plasmas has been studied for many years. Many details of such interaction were described (see, for example, Refs. [13–18] and references cited therein). However, the problem of influence of the finite sizes of particles on interaction forces still remains open. In the meanwhile, the knowledge of such influence is important for the correct description of dusty crystal formation and modeling of ordered structures in dusty plasma [19,20].

The purpose of the present paper is to study the influence of finite sizes of charged particles embedded into plasma-like medium on the interaction forces between two particles and to propose the description of such forces in terms of effective interactions. Since the objects under consideration (grains and charged colloidal particles) accumulate and carry very large electric charge and thus nonlinear effects should be taken into account, the problem was solved numerically. Dynamics of plasma was described in the drift-diffusion approximation that is applicable to the case of weakly ionized strongly collisional plasmas which takes place in dusty plasma experiments [21–23].

Notice that dusty plasmas and charged colloidal suspensions have many common features such as the similar composition, presence of highly charged macroparticles, ordered structure formation, etc. However, there is one very important difference between them which concerns the mechanism of macroparticle charging. In the case of charged colloidal suspensions, a macroparticle charge appears due to the chemical interaction of macroparticle with solvent. Such charge is fixed and we can assume no charge exchange between the colloidal particle and electrolyte. On the contrary, in the case of grain embedded into plasma, the grain charge appears as a result of electron and ion collection by grain [6]. Due to the electron-ion recombination on the surface of the grain, its charge is maintained by the permanent plasma particle fluxes towards the grain surface. This means that in such case the grain charge is dependent on the plasma dynamics and it should be calculated self-consistently with due regard of the presence of other grains. This introduces one more complication related

*momot.andriy@gmail.com
†azagorodny@bitp.kiev.ua
‡orlyninna@gmail.com

 

to the fact that the charge of solitary grain is different from that in the presence of the second grain, at least if they are located in the vicinity of each other. This problem is also studied in the present paper.

The paper is organized in the following order. The general statement of the problem and basic equations are formulated in Sec. II. This section also includes the description of the numerical method used for the solution of the problems under consideration. In Sec. III we discuss briefly the properties of the screening of solitary particles and recover some results, which are used to describe two-particle effects in the interaction of finite-size charged particles. The difference between the effective potentials for the case of particle without charge exchange with the surrounding plasma and particle charged by plasma currents is also discussed. The results of numerical studies of the interaction forces acting between two finite-size particles are presented in Sec. IV.

## II. STATEMENT OF THE PROBLEM AND BASIC EQUATIONS

Let us consider two charged spherical conducting macroparticles of the radius $a$ embedded into infinite strongly collisional, weakly ionized plasma. We assume that each particle has the charge $q$ and the distance between centers of the particles is equal to $2c$. The geometry of the system under consideration is shown in Fig. 1.

The force acting on one of the particles (for example, that with the coordinate $\mathbf{r} = \{0,0,c\}$) can be calculated on the basis of the following treatment. Let us consider the surface element $dS$. In the case of conducting particle its charge is $dq = \sigma dS$, where $\sigma$ is the surface charge density, which is the function of coordinate. The electric field strength $\mathbf{E}$ is directed along the normal to the surface and has the value $E = 4\pi\sigma$. The force acting on the surface element is given by

$$d\mathbf{F} = \sigma(\mathbf{E} - \mathbf{E}_S)dS, \tag{1}$$

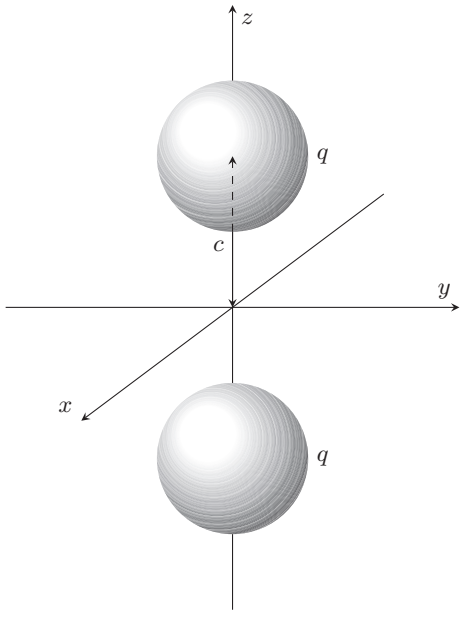


FIG. 1. Mutual displacement of particles and coordinate system.

where $\mathbf{E}_S$ is the electric field generated by the surface element

$$\mathbf{E}_S = 2\pi\sigma\mathbf{n}, \tag{2}$$

where $\mathbf{n}$ is the unit vector of the external normal to the surface element.

Thus, the force acting on it can be written as

$$d\mathbf{F} = 2\pi\sigma^2\mathbf{n}dS. \tag{3}$$

The total force is given by

$$\mathbf{F} = 2\pi\oint_S \sigma^2 d\mathbf{S} = \frac{1}{8\pi}\oint_S \left(\mathbf{n}\frac{\partial\varphi}{\partial\mathbf{r}}\right)^2 d\mathbf{S}. \tag{4}$$

In view of the cylindrical symmetry of the problem, we use a cylindrical coordinate system. In such a case, the surface of the particle $S$ is given by the equation $r_\perp^2 + (z-c)^2 = a^2$ and thus the normal to the surface can be written as $\mathbf{n} = \{\mathbf{r}_\perp/a, (z-c)/a\}$.

As is easy to see in the system under consideration, $\mathbf{F}$ has a nonzero $z$ component only:

$$F = F_z = \frac{1}{8\pi a}\oint_S \left(\mathbf{n}\frac{\partial\varphi}{\partial\mathbf{r}}\right)^2 (z-c)dS. \tag{5}$$

The potential $\varphi(\mathbf{r})$ satisfies the Poisson equation. In the case of singly ionized ions $e_i = -e_e = e$, where $e$ is elementary charge, one has

$$\Delta\varphi(\mathbf{r}) = 4\pi e[n_e(\mathbf{r}) - n_i(\mathbf{r})], \tag{6}$$

where $n_\alpha(\mathbf{r})$ is the density of the corresponding plasma particles species. This equation should be supplemented with the boundary conditions. In all the cases, the potential should decrease with the distance and thus

$$\varphi(\mathbf{r})\big|_{r\to\infty} = 0. \tag{7}$$

The boundary condition for the potential at the conducting particles surface is

$$\varphi(\mathbf{r})\big|_S = \varphi_S = \text{const}. \tag{8}$$

The way of estimating the $\varphi_S$, as well as the boundary condition for electrons and ions distributions around the particles, depends on the properties of macroparticles and should be treated separately.

In order to study the influence of surface charge polarization on the interaction of conductive particles, we also consider the interaction of macroparticles with uniform surface charge density $\sigma_0 = q/4\pi a^2$. In such a case, the $z$ component of the force acting on the surface element is given by

$$dF_z = \sigma_0 E_z dS \tag{9}$$

and the $z$ component of the force acting on entire surface is

$$F_z = -\frac{q}{4\pi a^2}\oint_S \frac{\partial\varphi}{\partial z}dS. \tag{10}$$

Electrostatic potential $\varphi(\mathbf{r})$ is generated by both charged macroparticles and surrounding plasma. The potential of macroparticle with uniform surface charge density has the spherical symmetry. Thus, the contribution into force (10) acting on considered macroparticle from its electric field is equal to zero.

In contrast to conducting particles, for the particles with uniform surface charge density the electric field inside the sphere is not equal to zero. Thus, one should solve the Poisson equation $\Delta\varphi_i(\mathbf{r}) = 0$ inside the sphere along with (6) outside. The boundary condition on the particle surface is

$$\mathbf{n}\frac{\partial\varphi}{\partial\mathbf{r}}\bigg|_S - \mathbf{n}\frac{\partial\varphi_i}{\partial\mathbf{r}}\bigg|_S = 4\pi\sigma_0. \tag{11}$$

### A. Macroparticles with no charge exchange with surrounding plasma

If there is no charge exchange between the macroparticles and plasma (such picture is observed in the case of charged colloidal suspensions) the value of $\varphi_S$ in boundary condition (8) should be taken in such a way that $\varphi(\mathbf{r})$ satisfies the Gauss's law

$$\oint_S \mathbf{n}\frac{\partial\varphi}{\partial\mathbf{r}}dS = -4\pi q, \tag{12}$$

where $q$ is the given charge of macroparticle.

The electron and ion densities can be approximated by the Boltzmann distribution

$$n_\alpha(\mathbf{r}) = n_0\, e^{-\frac{e_\alpha\varphi(\mathbf{r})}{T_\alpha}} \tag{13}$$

and thus Eq. (6) has the form of Poisson-Boltzmann equation

$$\Delta\varphi(\mathbf{r}) = 4\pi e n_0\big(e^{\frac{e\varphi(\mathbf{r})}{T_e}} - e^{-\frac{e\varphi(\mathbf{r})}{T_i}}\big). \tag{14}$$

In the dimensionless variables

$$\phi = \frac{e_e\varphi}{T_e}, \quad \tau = \frac{T_e}{T_i}, \quad \tilde{r} = \frac{r}{\lambda_D}, \tag{15}$$

where $\lambda_D$ is the Debye length,

$$\lambda_D = \frac{1}{k_D}, \quad k_D^2 = \sum_\alpha k_{D\alpha}^2, \quad k_{D\alpha}^2 = \frac{4\pi e_\alpha^2 n_0}{T_a},$$

the equation for the potential has the form

$$\Delta\phi(\tilde{\mathbf{r}}) = \frac{e^{\tau\phi(\tilde{\mathbf{r}})} - e^{-\phi(\tilde{\mathbf{r}})}}{1+\tau}. \tag{16}$$

### B. Grains charged by plasma currents

If a macroparticle (grain) absorbs all encountered electrons and ions, the surface value of the potential $\varphi_S$ is still fixed, but instead of (12) we have to take into account that the stationary value of the grain charge is determined by the total electric current through the grain surface,

$$I_{\text{tot}} = \sum_\alpha I_\alpha = \sum_\alpha e_\alpha \oint_S \mathbf{\Gamma}_\alpha d\mathbf{S} = 0, \tag{17}$$

where flux density $\mathbf{\Gamma}_\alpha$ satisfies the stationary continuity equation

$$\text{div}\mathbf{\Gamma}_\alpha(\mathbf{r}) = 0 \tag{18}$$

and boundary conditions for $n_\alpha(\mathbf{r})$, namely,

$$n_\alpha(\mathbf{r})|_S = 0, \tag{19}$$

$$n_\alpha(\mathbf{r})|_{r\to\infty} = n_0. \tag{20}$$

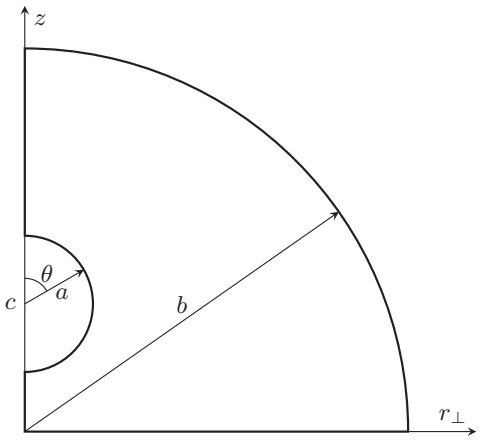


FIG. 2. Computation domain.

In the drift-diffusion approximation, which we apply for the description of plasma dynamics in the case of weakly ionized, strongly collisional plasma, the electron and ion flux densities are

$$\mathbf{\Gamma}_\alpha(\mathbf{r}) = -\mu_\alpha n_\alpha(\mathbf{r})\nabla\varphi(\mathbf{r}) - D_\alpha\nabla n_\alpha(\mathbf{r}). \tag{21}$$

Mobility $\mu_\alpha$ and diffusion coefficient $D_\alpha$ are gathered by the Einstein relation and can be expressed in terms of plasma particles' mean free path $l_\alpha$

$$\mu_\alpha = \frac{e_\alpha D_\alpha}{T_\alpha}, \quad D_\alpha = l_\alpha\sqrt{\frac{T_\alpha}{m_\alpha}}. \tag{22}$$

Using the dimensionless variables (15) and

$$\mathbf{G}_\alpha = \frac{\mathbf{\Gamma}_\alpha}{D_e n_0 k_D}, \tag{23}$$

one obtains

$$\begin{aligned}\mathbf{G}_e &= -\eta_e(\tilde{\mathbf{r}})\nabla\phi(\tilde{\mathbf{r}}) - \nabla\eta_e(\tilde{\mathbf{r}}),\\ \mathbf{G}_i &= (D_i/D_e)[\tau\eta_i(\tilde{\mathbf{r}})\nabla\phi(\tilde{\mathbf{r}}) - \nabla\eta_i(\tilde{\mathbf{r}})],\end{aligned} \tag{24}$$

where $\eta_\alpha = n_\alpha/n_0$ and thus the system of equations for the potential and plasma particles density has the form

$$\Delta\phi(\tilde{\mathbf{r}}) = \frac{\eta_i(\tilde{\mathbf{r}}) - \eta_e(\tilde{\mathbf{r}})}{1+\tau}, \tag{25}$$

$$\text{div}\mathbf{G}_\alpha(\tilde{\mathbf{r}}) = 0. \tag{26}$$

The problem of interaction between two spherical particles has the axial symmetry around the $z$ axis (see Fig. 1); thus in a cylindrical coordinate system, the potential is the function of two variables $\varphi(\mathbf{r}) = \varphi(r_\perp, z)$ as well as electron and ion number densities $n_\alpha(\mathbf{r}) = n_\alpha(r_\perp, z)$. The above-stated problems, which are two dimensional in $(r_\perp, z)$ coordinates, were solved numerically using the finite-element method. Taking into account the reflection symmetry with respect to $xy$ plane (Fig. 1) the computation domain shown in Fig. 2 was used. The boundary conditions (7) and (20) were approximated by the same conditions at $r = b$ in the computations, where $b \gg \lambda_D$. Normal components of $\nabla\phi(\tilde{\mathbf{r}})$, $\nabla\eta(\tilde{\mathbf{r}})$ to the boundaries $(z = 0, 0 < r_\perp < b)$, $(r_\perp = 0, 0 < z < c - a)$, and $(r_\perp = 0, c + a < z < b)$ are equal to zero, which corresponds

to the continuity of the potential, electron, and ion densities at these boundaries in view of the cylindrical and reflection symmetries of the problems.

The ratio of diffusion coefficients $D_e/D_i$ arises as a parameter after the normalization. Using the relation (22) $D_\alpha = l_\alpha\sqrt{T_\alpha/m_\alpha}$ and assuming plasma particle mean free path independence on temperature, one obtains $D_e/D_i = (l_e/l_i)\sqrt{m_i/m_e}\sqrt{T_e/T_i} = d\sqrt{\tau}$. Parameter $d$ is the ratio of the electron to ion diffusion coefficients in the case of isothermal plasma. The calculations were performed for $d = 1000$ (the same value was used in Refs. [24,25]) and $\tau = 1$ (isothermal plasma).

## III. EFFECTIVE POTENTIALS OF SOLITARY CHARGED MACROPARTICLE IN PLASMA

In order to clear up the two-particle effects in the problem of finite-size spherical conducting particles interaction, it is useful to compare the results of calculations with those following from the effective potential approximation. That is why we need to know the effective potential of solitary finite-sized charged particle.

With this purpose, we also solved Eq. (16) or Eqs. (25) and (26) with the boundary condition (7) or set of (7), (19), and (20) respectively. In view of the spherical symmetry of the problem in the case of one particle, the boundary condition at the particle surface is simplified to

$$\mathbf{n}\nabla\varphi(r)|_S = -\frac{q}{a^2}. \tag{27}$$

Along with the boundary condition (7), the latter condition is sufficient for the numerical solution of the boundary-value problem in the case of a particle which does not absorb electrons and ions from the surrounding plasma (in this case, the charge is treated as a given quantity). However, in the case of grain charged by plasma currents, the value of $q$ should be found self-consistently using the condition of zero electric current (17).

Since the effective potentials of charged finite-size particles are dependent on their absorptive properties it is reasonable to consider the case for particles with reflecting and absorbing surfaces separately.

### A. Macroparticle with reflecting surface (no exchange with the surrounding medium)

In this case we solve the Poisson-Boltzmann equation (16) with the boundary conditions (7) and (27) for isothermal plasma ($\tau = 1$). This problem was studied for many years, both analytically [26–31] and numerically [26,32,33]. In this section, for the sake of completeness, we recover some known results and add other numerical results. We start from the comparison of the numerical solution of the problem with the linearized solution, namely the Debye potential:

$$\varphi_D(r) = \frac{q}{r}\,e^{-k_D r}. \tag{28}$$

The ratios of the calculated potential to the Debye potential for various values of dimensionless macroparticle radii $a/\lambda_D$ and charges $z_g = qe_e/aT_e$ are presented in Figs. 3(a) and 3(b). These ratios differ from the constants only in the vicinity of the grain, which means that the particle potential can be well described by the Debye potential with the effective charge $q^{\text{eff}}$ that is defined by the constant values which approach the ratios. The notion of an effective charge comes from the work of Alexander *et al.* [26] and is developed in further studies.

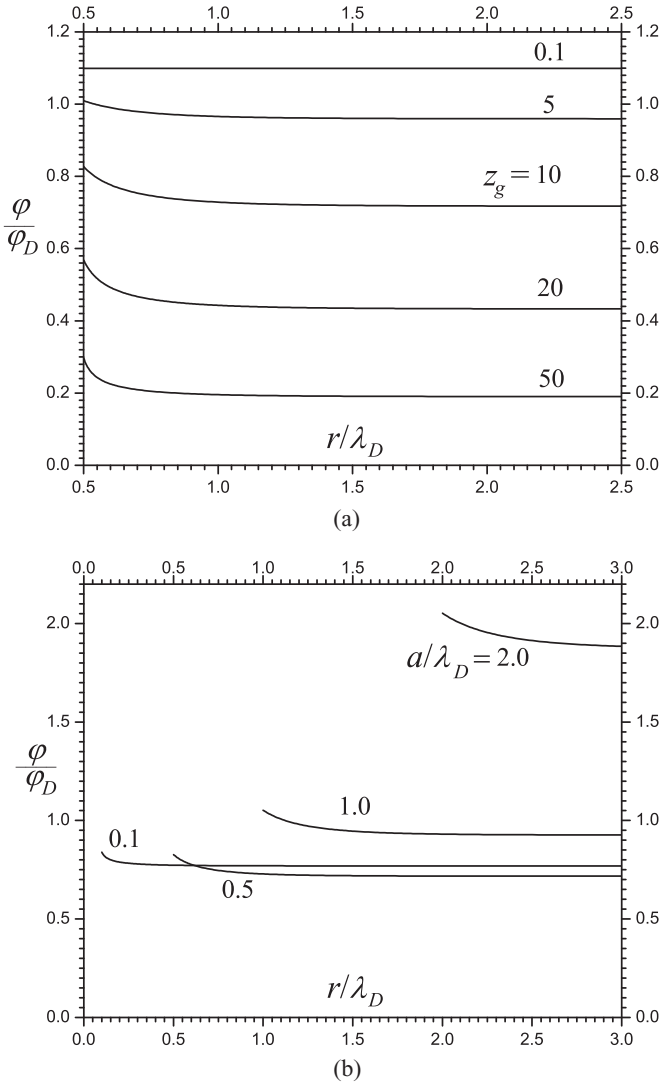


FIG. 3. Ratio of calculated potential to Debye potential $\varphi/\varphi_D$: (a) $a/\lambda_D = 0.5$, $z_g = 0.1,5,10,20,50$; (b) $z_g = 10$, $a/\lambda_D = 0.1,0.5,1.0,2.0$, $z_g = qe_e/aT_e$.

Figure 3(a) shows that for the fixed particle radius the growth of $z_g$ leads to the decrease of effective charge. The dependents of $q^{\text{eff}}$ on the particle radius for the fixed $z_g$ is slightly nonmonotonic [see Fig. 3(b)]. These conclusions are clearly illustrated in Fig. 4, where effective charge vs $z_g$ is plotted for various values of $a/\lambda_D$ and are in agreement with the results obtained in Ref. [32].

The analytic dependence of the effective charge on particle size can be taken from the Derjaguin-Landau-Verwey-Overbeek (DLVO) potential

$$q_D^{\text{eff}} = \frac{qe^{k_D a}}{k_D a + 1}, \tag{29}$$

which is obtained within the approximation $z_g \ll 1$.

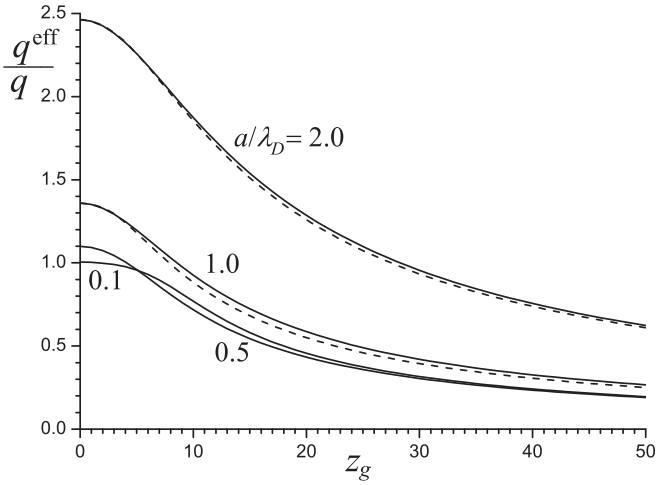


FIG. 4. Effective charge vs $z_g$ for $a/\lambda_D = 0.1, 0.5, 1.0, 2.0$; dashed lines correspond to (30).

One can see from Fig. 5 that $q_D^{\rm eff}$ is valid for any particle size while $z_g$ is less or equal to several units. For large values of $z_g$ the calculated effective charge is less than it is predicted by DLVO.

The following expression for the effective charge for $a/\lambda_D \gg 1$ can be found in [27,28,31]

$$\frac{q^{\rm eff}e_e}{aT_e} = \frac{e^{k_D a}}{k_D a + 1} t\left[4k_D a + 2\left(5 - \frac{t^4+3}{t^2+1}\right)\right], \tag{30}$$

where

$$t = T\left(\frac{z_g}{2k_D a + 2}\right), \quad T(x) = \frac{\sqrt{1+x^2}-1}{x}. \tag{31}$$

The analytical estimate for the effective charge (30), which is presented by dashed lines in Figs. 4 and 5, and numerical calculations are in agreement from $k_D a \approx 1$.

### B. Macroparticle with absorbing surface (dust grain)

It is known that in strongly collisional, weakly ionized plasma, grain potential has the Coulomb-like asymptote [6,24,34–36]

$$\varphi_{\rm asymp} = \frac{\tilde{q}}{r}, \tag{32}$$

where

$$\tilde{q} = -\frac{I}{k_D^2}\left(\frac{1}{D_i} - \frac{1}{D_e}\right) \tag{33}$$

and $I$ is the charging current.

To describe the grain potential at arbitrary distance, the sum of Debye and Coulomb potentials with effective charges can be used [35,37,38]. It was proposed in Ref. [36] to scale the screening length, namely to use the following expression:

$$\varphi_{0p}(r) = (q - \tilde{q})\frac{e^{-pk_D r}}{r} + \frac{\tilde{q}}{r}. \tag{34}$$

The parameter $p$ scales the screening length. It approaches unity only for $a \ll \lambda_D$ in isothermal plasma and sharply decreases with grain radius growth. In nonisothermal plasma, the value of $p$ is less than in isothermal plasma. Thus the screening length of a dust grain is much larger then the Debye radius. Formula (34) describes potential with maximum relative error of several percent as compared to numerical solution of Eqs. (24) and (25).

The grain charge $q$ and effective unscreened charge $\tilde{q}$ depend on grain size and the ratio of electron to ion temperature $T_e/T_i$. Their values can be found from numerical solution of the problem (the results of such solution obtained in Ref. [36] are presented in Fig. 6) or in the case of $a \ll \lambda_D$ from analytical expressions.

Approximate formulas for the potential were given also for weakly collisional regimes in Refs. [39,40], whose accuracy is confirmed by the numerical solution of the Bhatnagar–Gross–Krook (BGK) kinetic equation [41].

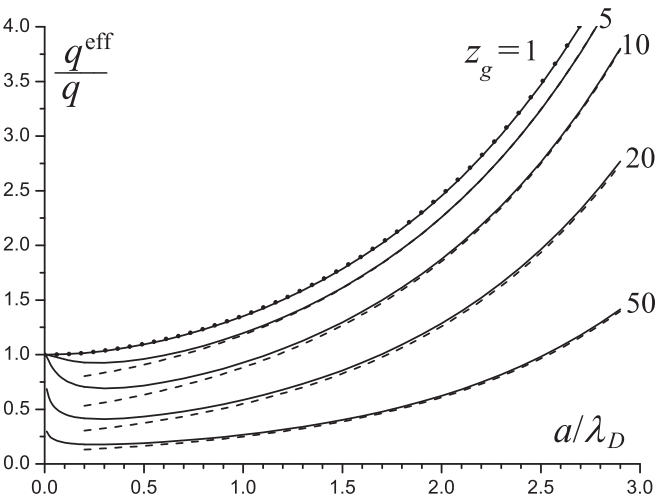


FIG. 5. Effective charge vs grain radius; lines are calculated for $z_g = 1, 5, 10, 20, 50$. Points correspond to DLVO effective charge (29); dashed lines correspond to (30).

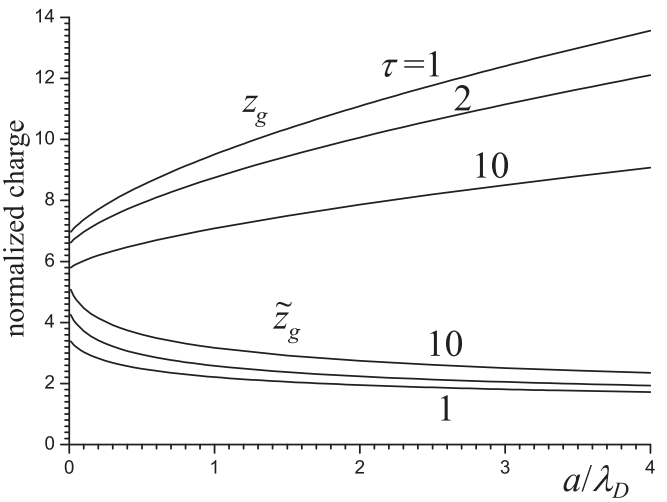


FIG. 6. Normalized grain charge $z_g = qe_e/aT_e$ and normalized unscreened charge $\tilde{z}_g = \tilde{q}e_e/aT_e$ in isothermal and nonisothermal ($\tau = T_e/T_i = 2, 10$) plasma vs grain radius.

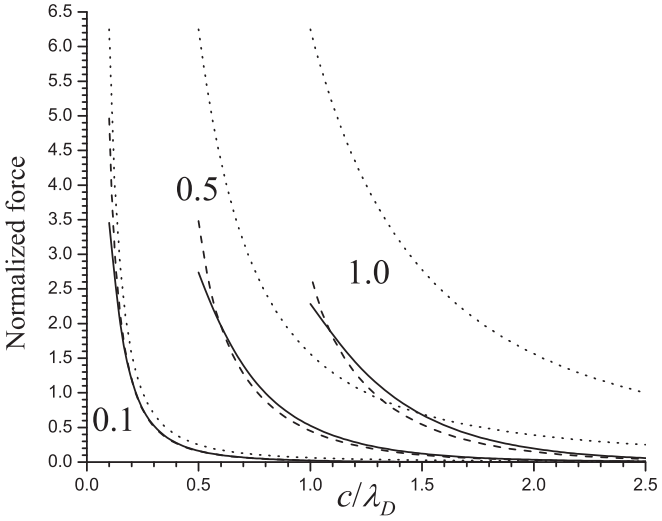


FIG. 7. Normalized repulsion force $F_z e^2/T_e^2$ between conducting particles (solid line), particles with fixed surface charge (dashed line), and $F_C$ (dotted line) vs half-distance between centers of the particles for $a = 0.1, 0.5, 1.0\lambda_D$, and $z_g = 5$.

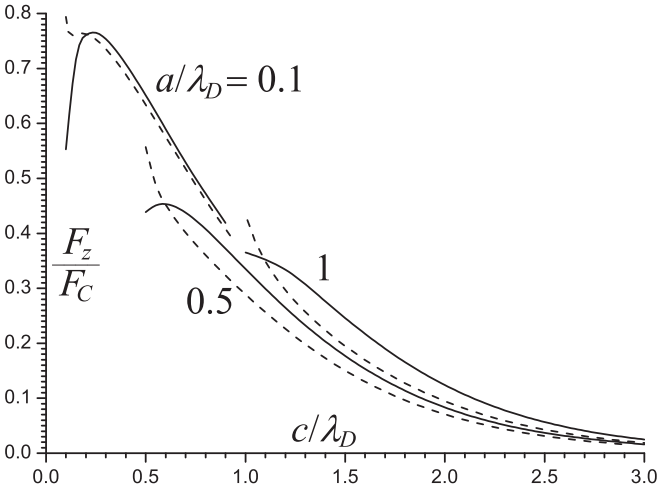


FIG. 8. The ratio of calculated force to the Coulomb force $F_z/F_C$ between conducting particles (solid line) and particles with fixed surface charge (dashed line) vs half-distance between centers of the particles for $a = 0.1, 0.5, 1.0\lambda_D$, and $z_g = 5$.

## IV. INTERACTION OF TWO CHARGED MACROPARTICLES IN PLASMA

In this section, we study the interaction of two charged spherical macroparticles of the same size in weakly ionized plasma.

### A. Macroparticles with reflecting surfaces (no exchange with the surrounding medium)

The results of numerical solution of Poisson-Boltzmann equation (14) are presented in this subsection.

The interaction force of two charged spherical particles in plasma within the Poisson-Boltzmann model were considered analytically in Ref. [42] using the Maxwell stress tensor and on the basis of electric field free energy. It was proven that the force is repulsive in both approaches in isothermal as well in nonisothermal plasma. Force was calculated via stress tensor also in Ref. [43].

In the present paper the forces $F_z$ acting on one particle from the other particle and induced charges in plasma are calculated by the formulas (5) and (10). Figure 7 shows the force versus half-distance between centers of the conducting macroparticles (solid line) and macroparticles with uniform surface charge density (dashed line). Various particles sizes $a = 0.1, 0.5, 1.0\lambda_D$ with same dimensionless charge $z_g = 5$ are considered. The Coulomb force of point charges in vacuum

$$F_C = \frac{q^2}{(2c)^2} \tag{35}$$

is represented by a dotted line in Fig. 7. Repulsion force decreases monotonically with distance growth. Obviously, the maximum repulsion force is reached when the macroparticles are in contact and the value of this maximum force decrease with macroparticle size growth.

It is evident that the interaction force between conducting particles and particles with uniform surface charge density in plasma-like medium is less than $F_C$ (see Fig. 7). In order to compare these forces, the ratio $F_z/F_C$ vs $c$ is found. The ratios for same value of $z_g = 5$ and various $a/\lambda_D = 0.1, 0.5, 1$ are presented in Fig. 8, and those for the same value of $a/\lambda_D = 0.5$ and various $z_g = 1, 5, 10$ are presented in Fig. 9. The ratio $F_z/F_C$ decreases rapidly with $c$ growth, and thus the screening of the macroparticle interaction takes place. The screening is less pronounced at short distances between macroparticles, where $F_z/F_C$ is higher, especially for smaller $a/\lambda_D$ and $z_g$. The interaction of charged macroparticles in plasma is close to the Coulomb law for $c \ll \lambda_D$, but such condition can be satisfied only for particles with radius much less than $\lambda_D$.

The values of forces between particles with uniform surface charge density and conducting particles are different. In

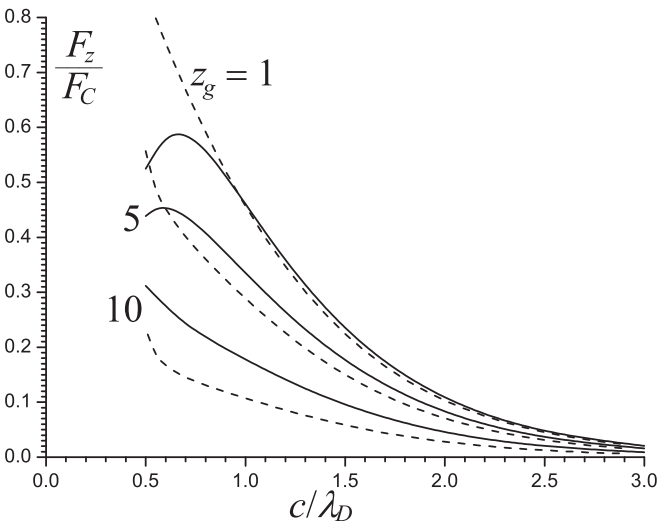


FIG. 9. The ratio of calculated force to the Coulomb force $F_z/F_C$ between conducting particles (solid line) and particles with fixed surface charge (dashed line) vs half-distance between centers of the particles for $a = 0.5\lambda_D$ and $z_g = 1,5,10$.

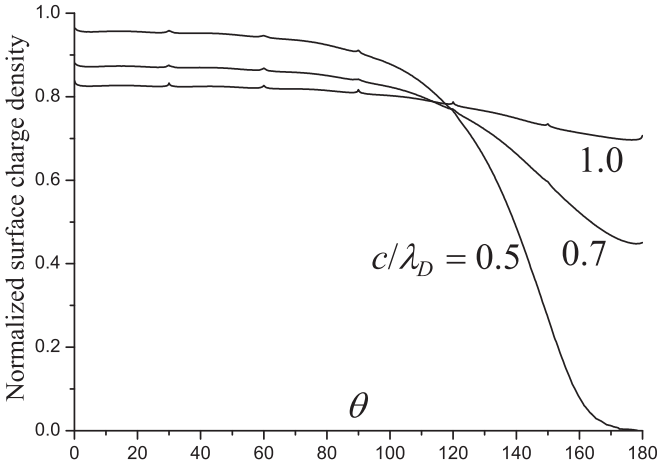


FIG. 10. Normalized surface charge density on conducting macroparticle $\sigma e_e/(T_e k_D)$ vs the $\theta$ angle (see Fig. 2) for $a = 0.5\lambda_D$, $z_g = 5$, and $c = 0.5, 0.7, 1\lambda_D$.

particular, when the particles are almost in contact $c \gtrsim a$, the force between conducting particles is less (the solid line is lower than the dashed line in Figs. 7–9 except for the case of $a/\lambda_D = 0.5, z_g = 10$ in Fig. 9). It is explained by the charge polarization on the surfaces of conducting macroparticles.

The polarization is clearly observed in Fig. 10. The normalized surface charge density $\sigma e_e/(T_e k_D)$ on conducting macroparticles of size $a = 0.5\lambda_D$ and charge $z_g = 5$ in the case of $c = 0.5\lambda_D$ is considerably less on the macroparticle sides facing each other than those on opposite sides and falls to the zero in the place of macroparticle contact. This leads to the reduction of repulsion force as compared to macroparticles with uniform surface charge density (see Fig. 8). For $c = 0.7\lambda_D$ the polarization is still considerable but less pronounced, and for $c = \lambda_D$ it can almost be neglected.

Figure 11 shows how the surface charge polarization depends on dimensionless charge $z_g$ for the particles in contact ($c/\lambda_D = 0.5$). The figure reveals that the polarization

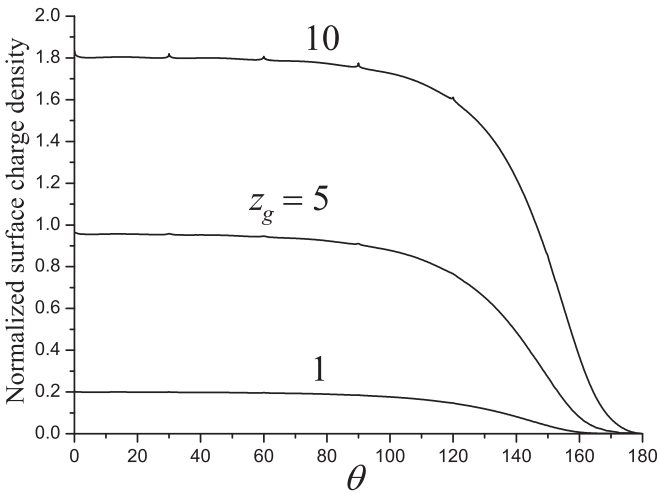


FIG. 11. Normalized surface charge density on conducting macroparticle $\sigma e_e/(T_e k_D)$ vs the $\theta$ angle (see Fig. 2) for $a = 0.5\lambda_D$, $c = 0.5\lambda_D$, and $z_g = 1, 5, 10$.

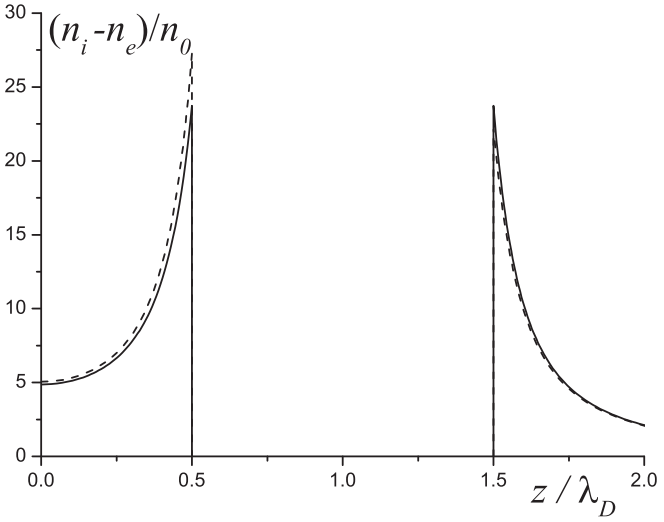


FIG. 12. Normalized charge density $(n_i - n_e)/n_0$ vs $z/\lambda_D$ near one of the two interacting conducting particles (solid line) or particles with fixed surface charge (dashed line) for $a = 0.5\lambda_D$, $c = \lambda_D$, and $z_g = 5$.

decreases as $z_g$ grows; in particular the region of almost zero value of surface charge is smaller for higher values of $z_g$. This fact explains behavior of curves in Fig. 9 for $c \gtrsim a$, namely that the repulsion force between conducting particles is considerably less than for particles with fixed surface charge (solid line is lower than dashed line) for $z_g = 1$. This effect is less pronounced for $z_g = 5$ and disappears for $z_g = 10$.

Also, one can see that the repulsion between conducting particles is higher than between particles with uniform surface charge density (solid line is higher than dashed line in Figs. 8, 9) except for the region of $c \ll \lambda_D$, which was discussed above. This fact is explained by Fig. 12, in which the normalized charge density distribution $(n_i - n_e)/n_0$ along the $z$ axis near one of the two interacting macroparticles of size $a = 0.5\lambda_D$ in plasma is depicted. The charge density is equal to zero inside the macroparticle ($0.5 \leqslant z \leqslant 1.5$). There are more positive charges between negatively charged macroparticles with uniform surface charge density as compared to conducting macroparticles (dashed line is higher than solid line in Fig. 12) and vice versa for $z > 1.5$. This results in the reduction of macroparticle repulsion. Thereby, the interaction of macroparticles significantly depends on surface charge properties, not only at short distance between macroparticles, where polarization is important, but at any distance.

Also, the comparison of calculated force with the one found from Debye potential

$$F_D = \left(\frac{q^{\text{eff}}}{2c}\right)^2 e^{-2ck_D}(1 + 2ck_D) \tag{36}$$

was made. Effective charge $q^{\text{eff}}$ depends on parameters $\tau$, $z_g$, and $a/\lambda_D$ [see Fig. 3(a)]. The values of $q^{\text{eff}}/q$ used in further calculations are presented in Table I.

The ratio $F_z/F_D$ for conducting particles of several values of $ak_D$ and $z_g$ versus half distance between centers $c$ is shown in Fig. 13 (minimal value of $c$ is equal to macroparticle radius). This ratio grows with distance and tends to one. It means

TABLE I. Ratio of effective to real charge $q^{\text{eff}}/q$.

| $a/\lambda_D$ | $z_g = 1$ | $z_g = 5$ | $z_g = 10$ |
|---|---|---|---|
| 0.1 | 1.0037 | 0.9569 | 0.7697 |
| 0.5 | 1.0929 | 0.9597 | 0.7176 |
| 1.0 | 1.3514 | 1.1961 | 0.9264 |

that the interaction is described with Debye force (36) with corresponding effective charge at distance $c \gg a$. For particles of different sizes $a = 0.1, 0.5, 1.0\lambda_D$ and the same $z_g = 5$ the value 10% of relative error of Debye force is reached at $c \approx 0.25, 1, 1.7\lambda_D$ respectively. At distance $c \approx a$ the ratio $F_z/F_D$ does not considerably depend on macroparticle radius for $z_g = 1{,}5$ and it is approximately 0.6. The dependence of relative error of Debye force on dimensionless macroparticle charge $z_g$ for the fixed $a/\lambda_D$ is ambiguous. On the one hand, the relative error decreases more rapidly with $c$ increase for smaller values of $z_g$, but on the other hand, when the macroparticles are almost in contact ($c \approx a$) the relative error is smaller for higher values of $z_g$. For $a = 0.5\lambda_D$ and $z_g = 10$ the relative error of Debye force does not exceed 20% in all range of macroparticle separation distance.

The ratio $F_z/F_D$ for macroparticles with uniform surface charge density of several values of $ak_D$ and $z_g$ is shown in Fig. 14. The ratio tends to constant value at certain distance between macroparticles, but this value is less the unity and decreases with macroparticle size and dimensionless charge growth. It means that as well as for conducting macroparticles the interaction at distance $c \gg a$ is described by the Debye force (36), but with other effective charges $q_2^{\text{eff}}$, which is determined by the constant value of ratio $F_z/F_D$. The values of $q_2^{\text{eff}}$ are presented in Table II and Fig. 15; according to them $q_2^{\text{eff}}$ is less than the effective charge $q^{\text{eff}}$ calculated for one macroparticle (see Fig. 5), but they have the same qualitative dependence on macroparticle radii.

If $q_2^{\text{eff}}$ is used as the effective charge in the Debye force (36) than the ratio $F_z/F_D$ approaches unit for $c \gg a$. The relative error of $F_D(q_2^{\text{eff}})$ does not exceed 15% for the given parameters;

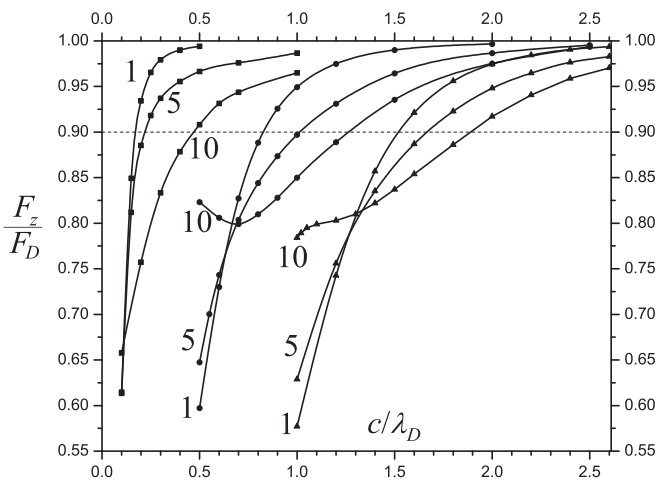


FIG. 13. The ratio of calculated force to (36) $F_z/F_D$ vs half-distance between centers of conducting macroparticles for $a = 0.1, 0.5, 1.0\lambda_D$, and $z_g = 1, 5, 10$.

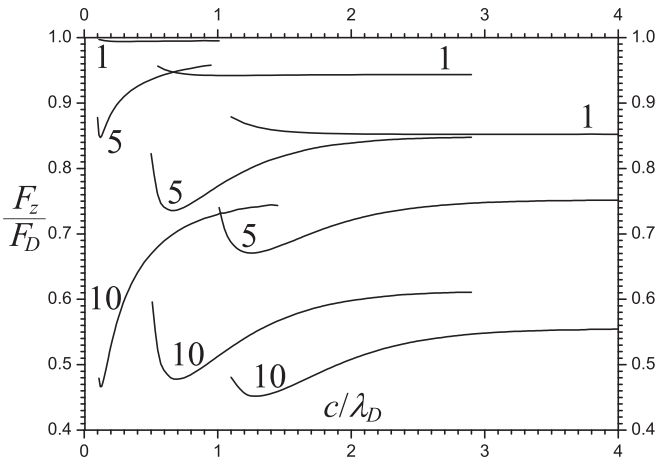


FIG. 14. The ratio of calculated force to (36) $F_z/F_D$ vs half-distance between centers of macroparticles with uniform charge density for $a = 0.1, 0.5, 1.0\lambda_D$, and $z_g = 1, 5, 10$.

thus the Debye force better describes the interaction of macroparticles with uniform surface charge distribution than the conductive macroparticles, of course, with corresponding effective charge.

### B. Macroparticles with absorbing surfaces (dust grains)

The repulsion force between two grains was calculated by formula (5). Note again that it is the force acting on surface charge of the grain from the electric field of other grain and induced charges in plasma. Forces versus half-distance between centers of the grains with radii $a = 0.1\lambda_D$ and $a = 0.5\lambda_D$ are presented in Figs. 16 and 17.

The interaction force can be obtained within the approximation that the second grain is pointlike and is situated in the field of the first grain, which is not disturbed by the first grain

$$F = -q\frac{d\varphi}{dr}, \tag{37}$$

where $\varphi$ is the effective potential of a singe grain in plasma; such potentials were considered in Subsec. III B. Using the fact that potential asymptotic behavior is Coulomb-like [see Eq. (32)], Eq. (37) gives

$$F = q\frac{\tilde{q}}{(2c)^2}, \tag{38}$$

or in the normalized form

$$\frac{Fe^2}{T_e^2} = z_g\tilde{z}_g\left(\frac{a}{2c}\right)^2. \tag{39}$$

The values of grain charge $z_g$ and unscreened charge $\tilde{z}_g$ can be taken from the calculations for the single grain; namely, they

TABLE II. Ratio of effective to real charge $q_2^{\text{eff}}/q$.

| $a/\lambda_D$ | $z_g = 1$ | $z_g = 5$ | $z_g = 10$ |
|---|---|---|---|
| 0.1 | 1.0013 | 0.937 | 0.664 |
| 0.5 | 1.0616 | 0.883 | 0.561 |
| 1.0 | 1.2477 | 1.037 | 0.689 |

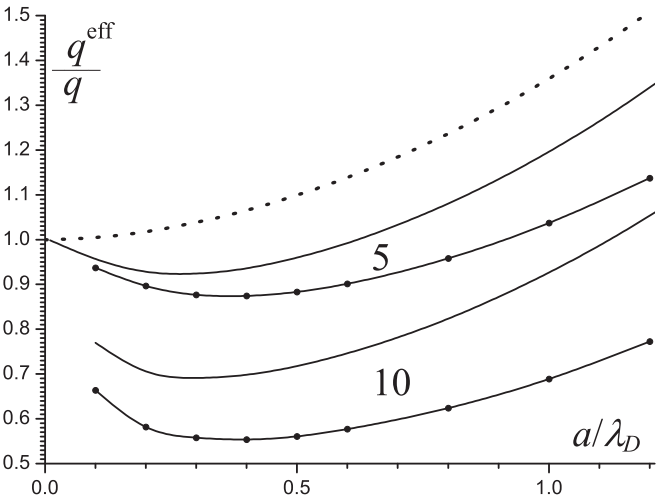


FIG. 15. Effective charge vs grain radius for $z_g = 5$ and 10. Points correspond to DLVO effective charge (29), the solid line is the effective charge calculated for one macroparticle (Fig. 5), and the line with circles is $q_2^{\rm eff}$ for the interaction of macroparticles with uniform surface charge.

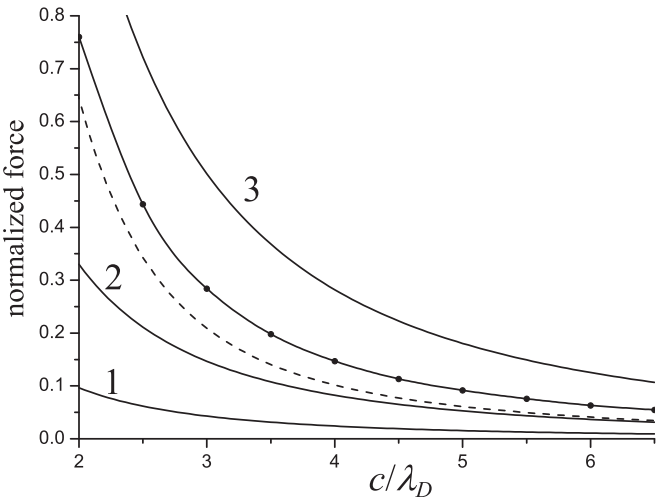


FIG. 17. Normalized repulsion force $Fe^2/T_e^2$ between two grains with radii $a = 0.5\lambda_D$ vs half-distance between centers of the grains $c/\lambda_D$: the line with circles is calculated; line 1–$\tilde{q}^2/(2c)^2$, 2–$q\tilde{q}/(2c)^2$, 3–$q^2/(2c)^2$; and the dashed line is obtained from (37) using the calculated potential $\varphi$ of the single grain.

are $z_g \approx 7.371$, $\tilde{z}_g \approx 3.021$ for $a = 0.1\lambda_D$ and $z_g \approx 8.496$, $\tilde{z}_g \approx 2.485$ for $a = 0.5\lambda_D$ (see Fig. 6 or Ref. [36]). The force given by formula (39) is presented in Figs. 16 and 17 by line 2, which is the closest to calculated curve as compared to forces $q^2/(2c)^2$ (line 3) and $\tilde{q}^2/(2c)^2$ (line 1). The values given by (39) are less than calculated force values, and the difference is more considerable for the grains of size $a = 0.5\lambda_D$. It is possible to assume that (39) underestimates the force due to insufficient precision of (32), but the dashed line, which is obtained from (37) using the calculated effective potential $\varphi$ of the single grain [36], shows almost the same difference with calculated force at $c \gg \lambda_D$ as (39). Thus, it can be explained by the two-particle and/or size effects. It can be concluded that the expression (38) describes qualitatively the repulsion between grains only with radii much less than Debye length ($a \ll \lambda_D$) for $c \gg \lambda_D$.

Let us compare the calculated force with the Coulomb one $F_C = q^2/(2c)^2$, as was done in Subsec. IV A. The ratios $F_z/F_C$ are plotted in Fig. 18 for three values of grain radii $a = 0.1, 0.5, 1.0\lambda_D$. These ratios tend to constant value $\approx$0.5 at large distances between grains ($c \gg \lambda_D$). It means that for considered parameters the interaction force between two grains is twice less then the Coulomb force and can be asymptotically described by

$$\frac{1}{2}F_C = \frac{1}{2}\frac{q^2}{(2c)^2}. \tag{40}$$

Thus, the interaction force is not described quantitatively by the single grain potential even at large distances between grains (except the case of $a \ll \lambda_D$). Similarly to the case

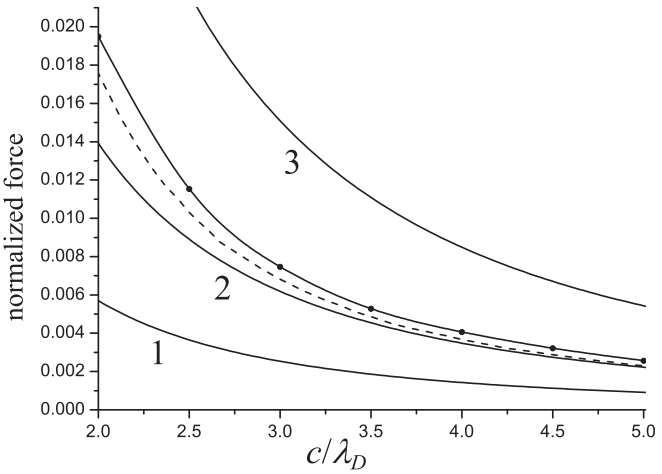


FIG. 16. Normalized repulsion force $Fe^2/T_e^2$ between two grains with radii $a = 0.1\lambda_D$ vs half-distance between centers of the grains: the line with circles is calculated; line 1 corresponds to $\tilde{q}^2/(2c)^2$, 2–to $q\tilde{q}/(2c)^2$, 3–to $q^2/(2c)^2$; and the dashed line is obtained from (37) using the calculated potential $\varphi$ of the single grain.

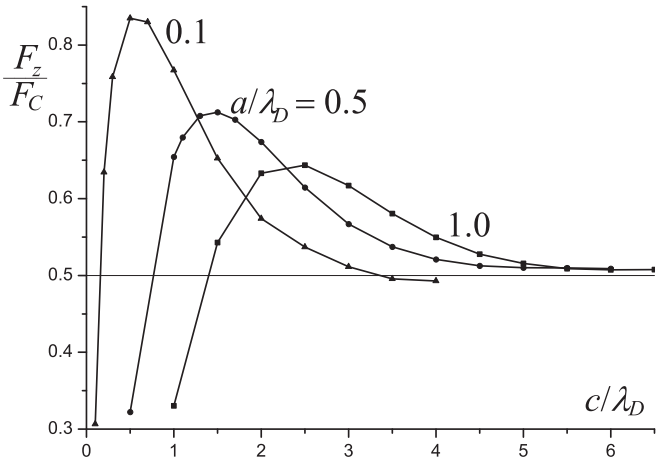


FIG. 18. Ratio of calculated force to the Coulomb force (35) $F_z/F_C$ vs half-distance between centers of the grains for $a/\lambda_D = 0.1, 0.5, 1.0$.

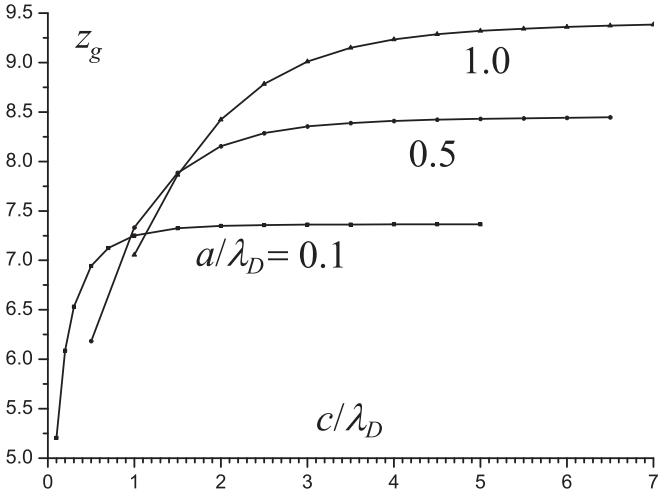


FIG. 19. Normalized grain charge $z_g = qe_e/aT_e$ vs half-distance between centers of the grains for $a/\lambda_D = 0.1, 0.5, 1.0$.

of nonabsorbing macroparticles with uniform surface charge density (see Subsec. IV A), the potential of the single particle gives the correct distance dependence of the force, but the correct quantitative description demands the introduction of some effective charge, which in case of two grains is $\tilde{q}^{\text{eff}} = q/2$.

The ratios $F_z/F_C$ nonmonotonically depend on distance between grains; they grow with $c$ decrease and after reaching the maximum values they rapidly decrease. The growth of $F_z/F_C$ is explained by the contribution to the force from the Debye part of the grain potential (34).

At close distance between grains, their mutual influence is the strongest. One effect of this influence is the considerable decrease of grain charges with $c$ decrease, which is depicted by Fig. 19. The charge decrease in turn is related to the decrease of charging currents [44]. Another effect is the charge polarization on the surfaces of grains. Both these effects lead to the decrease of repulsion force as compared to the Coulomb one.

## V. CONCLUSIONS

The influence of two-particle effects on interaction force between two charged spherical conducting macroparticles in isothermal plasma-like medium is studied. The calculations were performed for macroparticles which do not exchange charges with environment (colloidal particles in charged colloidal suspensions), as well as for macroparticles which are charged due to absorption of electrons and ions from surrounding plasma (grains in dusty plasma). In order to reveal the two-particle contribution into interaction force, the effective potentials of single particles were calculated. It was recovered that the potential distribution of colloidal particle is well described by the Debye potential with effective charge and the grain potential has Coulomb-like asymptotic behavior with effective charge, which is about one half of the real charge for $a \ll \lambda_D$ and decreases with particle-size growth. The dependence of effective charge on particles radii are studied.

The interaction forces were found from the direct calculations of the potential distribution in the presence of two macroparticles and compared with those obtained on the basis of the effective potential, assuming that the second macroparticle is sizeless. The comparison shows that at the distances of several particle sizes, the interaction force between two conducting macroparticles, which do not exchange charges with the environment, can be quantitatively described by the force obtained from the Debye potential. But in the case of particles with uniform surface charge density distribution, the effective charge is distinct (less) to effective charge of single particle. For smaller distances the deviation between the calculated force and the force obtained from the Debye potential decreases and reaches ≈40% when particles are in contact.

Two-particle effects are especially essential for the description of grain interaction. The interaction force is approximately equal to the half of the Coulomb force of pointlike particles with corresponding charges at distance $c \gg \lambda_D$ and considered parameters. It means that the effective interaction charge is approximately equal to the half of total particle charge independently on $a/\lambda_D$. At distance of several $a$, the polarization effects and considerable decrease of grain total charge is observed. Thus, in order to calculate the interaction force between two macroparticles at small and intermediate distances the self-consistent system of equations for electric potential, particle distributions, and grain charge should be used.

[1] P. W. Thomson, Philos. Mag. Series 4 **5**, 287 (1853).
[2] V. A. Saranin, Phys. Usp. **42**, 385 (1999).
[3] J. Lekner, Proc. R. Soc. London, Ser. A **468**, 2829 (2012).
[4] K. Kolikov, D. Ivanov, G. Krastev, Y. Epitropov, and S. Bozhkov, J. Electrost. **70**, 91 (2012).
[5] V. N. Tsytovich, Phys. Usp **40**, 53 (1997).
[6] V. Fortov, A. Ivlev, S. Khrapak, A. Khrapak, and G. Morfill, Phys. Rep. **421**, 1 (2005).
[7] P. Pieranski, Phys. Rev. Lett. **45**, 569 (1980).
[8] J. Derksen and W. van de Water, Phys. Rev. A **45**, 5660 (1992).
[9] M. Hoppenbrouwers and W. van de Water, Phys. B (Amsterdam, Neth.) **228**, 153 (1996).
[10] M. Hoppenbrouwers and W. van de Water, Phys. Rev. Lett. **80**, 3871 (1998).
[11] H. Thomas, G. E. Morfill, V. Demmel, J. Goree, B. Feuerbacher, and D. Möhlmann, Phys. Rev. Lett. **73**, 652 (1994).
[12] J. H. Chu and Lin I, Phys. Rev. Lett. **72**, 4009 (1994).
[13] M. Markes and P. Williams, Phys. Lett. A **278**, 152 (2000).
[14] A. N. Starostin, A. V. Filippov, A. F. Pal, A. I. Momot, and A. G. Zagorodny, Contrib. Plasm. Phys. **47**, 388 (2007).
[15] A. V. Filippov, A. G. Zagorodny, A. I. Momot, A. F. Pal', and A. N. Starostin, J. Exp. Theor. Phys. **105**, 831 (2007).
[16] H. Itou, T. Amano, and M. Hoshino, Phys. Plasmas **21**, 123707 (2014).

[17] M. Lampe and G. Joyce, Phys. Plasmas **22**, 023704 (2015).
[18] A. Davletov, L. Yerimbetova, Y. Mukhametkarimov, and A. Ospanova, Contrib. Plasm. Phys. **55**, 180 (2015).
[19] O. S. Vaulina, X. G. Koss, Y. V. Khrustalyov, O. F. Petrov, and V. E. Fortov, Phys. Rev. E **82**, 056411 (2010).
[20] P. Tolias, S. Ratynskaia, and U. de Angelis, Phys. Rev. E **90**, 053101 (2014).
[21] A. Pal', A. Serov, A. Starostin, A. Filippov, and V. Fortov, J. Exp. Theor. Phys. **92**, 235 (2001).
[22] V. Babichev, A. Pal', A. Starostin, A. Filippov, and V. Fortov, J. Exp. Theor. Phys. **80**, 241 (2004).
[23] A. Filippov, V. Babichev, N. Dyatko, A. Pal', A. Starostin, M. Taran, and V. Fortov, J. Exp. Theor. Phys. **102**, 342 (2006).
[24] O. Bystrenko and A. Zagorodny, Phys. Rev. E **67**, 066403 (2003).
[25] A. I. Momot, Phys. Plasmas **20**, 073703 (2013).
[26] S. Alexander, P. M. Chaikin, P. Grant, G. J. Morales, P. Pincus, and D. Hone, J. Chem. Phys. **80**, 5776 (1984).
[27] I. A. Shkel, O. V. Tsodikov, and M. T. Record, J. Phys. Chem. B **104**, 5161 (2000).
[28] M. Aubouy, E. Trizac, and L. Bocquet, J. Phys. A: Math. Gen. **36**, 5835 (2003).
[29] L. G. D'yachkov, Phys. Lett. A **340**, 440 (2005).
[30] V. I. Vishnyakov, G. S. Dragan, and V. M. Evtuhov, Phys. Rev. E **76**, 036402 (2007).
[31] L. Samaj and E. Trizac, J. Phys. A: Math. Theor. **48**, 265003 (2015).
[32] O. Bystrenko and A. Zagorodny, Phys. Lett. A **255**, 325 (1999).
[33] A. V. Shavlov, S. N. Romanyuk, and V. A. Dzhumandzhi, Phys. Plasmas **20**, 023703 (2013).
[34] C. H. Su and S. H. Lam, Phys. Fluids **6**, 1479 (1963).
[35] A. Filippov, A. Zagorodny, A. Momot, A. Pal, and A. Starostin, J. Exp. Teor. Phys. **104**, 147 (2007).
[36] A. Momot and A. Zagorodny, EPL **114**, 65004 (2016).
[37] A. Zagorodny, A. Filippov, A. Pal, A. Starostin, and A. Momot, J. Phys. Stud. **11**, 158 (2007).
[38] S. A. Khrapak, G. E. Morfill, V. E. Fortov, L. G. D'yachkov, A. G. Khrapak, and O. F. Petrov, Phys. Rev. Lett. **99**, 055003 (2007).
[39] A. Zagorodny, A. Momot, A. Filippov, A. Pal, and A. Starostin, Ukr. J. Phys. **54**, 1089 (2009).
[40] S. A. Khrapak, B. A. Klumov, and G. E. Morfill, Phys. Rev. Lett. **100**, 225003 (2008).
[41] I. Semenov, A. Zagorodny, and I. Krivtsun, Phys. Plasmas **19**, 043703 (2012).
[42] A. V. Filippov, A. F. Pal', A. N. Starostin, and A. S. Ivanov, JETP Lett. **83**, 546 (2006).
[43] S. L. Carnie, D. Y. Chan, and J. Stankovich, J. Colloid Interf. Sci. **165**, 116 (1994).
[44] A. I. Momot, Phys. Scr. **T161**, 014002 (2014).